DOI: 10.1021/ma100616f

Macromolecules
ARTICLE

Novel Silafluorene-Based Conjugated Polymers with Pendant Acceptor Groups for High Performance Solar Cells

Chunhui Duan, Wanzhu Cai, Fei Huang,* Jie Zhang, Ming Wang, Tingbin Yang, Chengmei Zhong, Xiong Gong, and Yong Cao*

Institute of Polymer Optoelectronic Materials & Devices, Key Laboratory of Specially Functional Materials of the Ministry of Education, South China University of Technology, Guangzhou 510640, P. R. China

Received March 21, 2010; Revised Manuscript Received May 7, 2010

ABSTRACT: Two low-band-gap conjugated polymers, PSiFDCN and PSiFDTA, which consist of alternating silafluorene and triphenylamine backbone and different pendant acceptor groups (malononitrile and 1,3-diethyl-2-thiobarbituric acid) with styrylthiophene as π-bridge, were synthesized and characterized. By changing the acceptor groups in side chain, the energy levels, absorption spectra, and band gaps of the resulted polymers were effectively tuned. As the strength of the acceptors increases, the band gap reduces from 1.83 eV for PSiFDCN to 1.74 eV for PSiFDTA. Bulk heterojunction solar cells with these polymers as electron donor and (6,6)-phenyl-C_{71}-butyric acid methyl ester ($PC_{71}BM$) as electron acceptor exhibit high V_{oc} (> 0.85 V) and power conversion efficiency (PCE) of 2.50% and 3.15% for PSiFDCN and PSiFDTA, respectively.

Introduction

Polymeric solar cells (PSCs) have attracted considerable attention over the past several years due to their unique advantages of low cost, light weight, and their potential for making flexible large area devices.[1−6] The most extensively used configuration of PSCs is the so-called "bulk heterojunction" devices, which involves the use of a phase-separated blend of an electron-donating conjugated polymer and an electron-accepting fullerene derivative such as (6,6)-phenyl-C_{61}-butyric acid methyl ester ($PC_{61}BM$) or (6,6)-phenyl-C_{71}-butyric acid methyl ester ($PC_{71}BM$) as the active layer.[1,7] Therefore, polymers with low band gaps, which can harvest more sunlight in the whole solar spectrum, have been widely used to enhance the efficiency of PSCs.[8−10] Despite a lot of advantages, the low power conversion efficiency (PCE) compared to commercial inorganic solar cells retarded the practical application of PSCs. Several factors are responsible for the low PCE of PSCs from a view of materials: first, the mismatch between the absorption spectrum of the photoactive layer and the terrestrial solar radiation, which leads to low short-circuit current density (J_{sc}); second, the relatively high highest occupied molecular orbital (HOMO) energy level of the polymers, which limits the magnitude of the open-circuit voltage (V_{oc}).[11] Several groups have reported that PSCs based on several different low-band-gap polymers with high J_{sc} due to their broad and strong absorption and accordingly PCE over 5%.[12−17] However, the V_{oc} of these PSCs are relatively low due to their high HOMO energy levels. On the other hand, PSCs with PCE as high as ∼4−5% have been achieved along with a high V_{oc} of ∼0.8−1.0 V by some groups by using polymers with a deep HOMO level but a relatively large band gap.[18−21] To realize the higher PCE of PSCs, it is still challenging to design and synthesize low-band-gap materials not only with strong and broad absorption to maximize J_{sc} but also with preferred energy levels to gain a high V_{oc}.[11]

*Corresponding authors. E-mail: msfhuang@scut.edu.cn (F.H.), poycao@scut.edu.cn (Y.C.).

To overcome this dilemma, one possible strategy is to design and synthesize two-dimensional conjugated polymers, in which the acceptors are located at the ends of the side chains and connected with donors on the electron-rich backbone through a π-bridge.[22] The absorption band and energy levels of the resultant conjugated copolymers could be fine-tuned by changing the acceptors in the side chain. Moreover, the two-dimensional conjugated structure may improve the isotropic charge transport of these type of polymer, which is important for PSCs.[23−26] As a result, the two-dimensional conjugated polymers based on polyfluorene derivatives exhibit excellent photovoltaic properties with a PCE as high as 4.74%.[22]

It has been proved that the bridging atom on the main chain of the conjugated polymers would greatly influence the properties of the materials.[13,18,27−30] It was reported the crystallinity of the silole-containing materials could be effectively improved compared to their carbon counterparts, which results in a better charge transport and might be also responsible for the reduced bimolecular recombination.[31,32] Hence, silole-containing conjugated polymers have been extensively applied in PSCs. For instance, by replacing the carbon atoms on the 7-position of the cyclopenta[2,1-*b*:3,4-*b*′]dithiophene with silicon atoms, an improved PCE from 3.2% to 5.1% was obtained from poly-[(4,4′-bis(2-ethylhexyl)dithieno[3,2-*b*:2′,3′-*d*]silole)-2,6-diyl-*alt*-(2,1,3-benzothiadiazole)-4,7-diyl] (PSBTBT).[13] Besides, when the carbon atoms on the 9-position of the fluorene moieties of the poly[2,7-(9-(2′-ethylhexyl)-9-hexylfluorene)-*alt*-5,5-(4′,7′-di-2-thienyl-2′,1′,3′-benzothiadiazole)] PFDTBT were replaced with silicon atoms, a higher efficiency of 5.4% was achieved from poly[(2,7-dioctylsilafluorene)-2,7-diyl-*alt*-(4,7-bis(2-thienyl)-2,1,3-benzothiadiazole)-5,5′-diyl] (PSiFDBT).[18] Additionally, silole-containing conjugated polymers have similar electronic structure to their carbon analogues, such as a deep HOMO level, which is the prerequisite for achieving high V_{oc}.[11] For example, when utilized as donor materials in PSCs, PSiFDBT demonstrated a high V_{oc} of 0.9 V, which is comparable to its carbon counterpart, PFDTBT.[18,28] Based on the considerations

 Published on Web 05/19/2010

mentioned above, the combination of the outstanding properties of silole and the advantages of two-dimensional conjugated polymers may develop a series of promising donor materials for high-performance PSCs.

In this paper, we report the synthesis and characterization of two new silafluorene-based two-dimensional conjugated polymers, PSiFDCN and PSiFDTA. Among them, the conjugated backbones consist of alternating conjugated silafluorene and triphenylamine units, and the acceptors of the polymers are linked with triphenylamine donors through a styrylthiophene π-bridge at the ends of the side chains. Photovoltaic properties of these polymers were investigated by fabricating bulk heterojunction photovoltaic devices using these polymers as electron donor and $PC_{71}BM$ as the acceptor. Both of them exhibited good device performance with high V_{oc} (>0.85 V) and PCE of 2.50% and 3.15% for PSiFDCN and PSiFDTA, respectively.

Experimental Section

Materials. 2,7-Bis(4,4,5,5-tetramethyl-1,3,2-dioxaborolan-2-yl)-9,9-dioctylsilafluorene[33,34] and 2-[2-[4-[*N*,*N*-di(4-bromophenyl)amino]phenyl]ethenyl]thien-5-al[22] were prepared according to the reported methods. Malononitrile and 1,3-diethyl-2-thiobarbituric acid were purchased from Sigma-Aldrich Chemical Co., $Pd(PPh_3)_4$ was purchased from Alfa Aesar Chemical Co., and they were used as received. All the solvents used were further purified prior to use. The other materials were common commercial level and used as received.

Synthesis of PSiFCHO. 2,7-Bis(4,4,5,5-tetramethyl-1,3,2-dioxaborolan-2-yl)-9,9-dioctylsilicafluorene (M1) (0.329 g, 0.500 mmol), 2-[2-[4-[*N*,*N*-di(4-bromophenyl)amino]phenyl]-ethenyl]thien-5-al (M2) (0.270 g, 0.500 mmol), and $Pd(PPh_3)_4$ (5 mg) were dissolved in a mixture of toluene (5 mL), tetrahydrofuran (THF) (5 mL), and sodium carbonate (1.0 M in water, 4 mL) in a 25 mL two-necked round-bottomed flask under argon. The mixture was refluxed with vigorous stirring in the dark for 7 h under an argon atmosphere. After cooling to room temperature, the mixture was poured into methanol. The precipitated material was collected by filtration through a funnel. After washing with acetone for 24 h in a Soxhlet apparatus to remove oligomers and catalyst residues, the resulting material was dissolved in 30 mL of chloroform. The solution was filtered with a 0.45 μm PTFE filter, concentrated, and precipitated from methanol to yield PSiFCHO as an orange solid (320 mg, 82%). ^{1}H NMR ($CDCl_3$, ppm): 9.85 (s, 1H), 7.89−7.85 (m, 4H), 7.75−7.60 (m, 7H), 7.41−7.39 (m, 3H), 7.19−6.84 (m, 8H), 1.49−1.40 (m, 4H), 1.25−1.19 (m, 24H), 0.88 (t, 6H). GPC (THF, polystyrene standard) M_n = 10.2 kg mol^{-1}, M_w = 30.3 kg mol^{-1}, PDI = 2.98. Anal. Calcd for $(C_{53}H_{57}NOSSi)_n$ (%): C, 81.12; H, 7.27; N, 1.79; S, 4.08. Found (%): C, 79.48; H, 7.63; N, 1.84; S, 4.23.

Synthesis of PSiFDCN. To a solution of PSiFCHO (100 mg, 0.13 mmol) and malononitrile (344 mg, 5.2 mmol) in 10 mL of chloroform was added 0.5 mL of pyridine. The mixture solution was stirred in the dark for 2 days at room temperature, after which the resulting mixture was poured into methanol and the precipitate was filtered off. The resulted polymer was dissolved in 20 mL of chloroform. The solution was filtered through a 0.45 μm PTFE filter, concentrated, and precipitated from methanol to yield the polymer as a black solid (87 mg, 81%). ^{1}H NMR ($CDCl_3$, ppm): 7.83−7.80 (m, 2H), 7.74 (s, 1H), 7.64−7.61 (m, 9H), 7.42−7.40 (m, 2H), 7.37−7.33 (m, 3H), 7.19−7.15 (m, 6H), 1.49−1.40 (m, 4H), 1.25−1.19 (m, 24H), 0.88 (t, 6H). GPC (THF, polystyrene standard): M_n = 11.5 kg mol^{-1}, M_w = 31.0 kg mol^{-1}, PDI = 2.69. Anal. Calcd for $(C_{56}H_{57}N_3SSi)_n$ (%): C, 80.77; H, 6.85; N, 5.05; S, 3.85. Found (%): C, 77.90; H, 7.08; N, 4.75; S, 3.79.

Synthesis of PSiFDTA. To a solution of PSiFCHO (100 mg, 0.13 mmol) and 1,3-diethyl-2-thiobarbituric acid (520 mg, 2.6 mmol) in 10 mL of chloroform was added 0.5 mL of pyridine. The mixture solution was stirred in the dark for 2 days at room temperature, after which the resulting mixture was poured into methanol and the precipitate was filtered off. The resulted polymer was dissolved in 20 mL of chloroform. The solution was filtered through a 0.45 μm PTFE filter, concentrated, and precipitated from methanol to yield the polymer as a black solid (116 mg, 91%). ^{1}H NMR ($CDCl_3$, ppm): 8.62 (s, 1H), 7.87−7.81 (m, 3H), 7.72−7.58 (m, 9H), 7.50−7.39 (m, 3H), 7.38−7.30 (m, 4H), 7.23−7.20 (m, 3H), 4.60 (m, 4H), 1.68 (t, 6H), 1.49−1.40 (m, 4H), 1.25−1.19 (m, 24H), 0.88 (t, 6H). GPC (THF, polystyrene standard): M_n = 12.3 kg mol^{-1}, M_w = 34.8 kg mol^{-1}, PDI = 2.83. Anal. Calcd for $(C_{61}H_{67}N_3O_2S_2Si)_n$ (%): C, 75.78; H, 6.94; N, 4.35; S, 6.63. Found (%): C, 70.95; H, 6.98; N, 4.63; S, 6.68.

Measurement and Characterization. ^{1}H NMR spectra were recorded on a Bruker AV-300 (300 MHz) in deuterated chloroform solution. Number-average (M_n) and weight-average (M_w) molecular weights were determined by a Waters GPC 2410 in THF using a calibration curve with standard polystyrene as a reference. Elemental analyses were performed on a Vario EL elemental analysis instrument (Elementar Co.). Differential scan calorimetry (DSC) measurements were performed on a Netzsch DSC 204 under N_2 flow at heating and cooling rates of 10 °C min^{-1}. Thermogravimetric analyses (TGA) were performed on a Netzsch TG 209 under N_2 flow at a heating rate of 10 °C min^{-1}. UV−vis absorption spectra were recorded on a HP 8453 spectrophotometer. Cyclic voltammetry (CV) was performed on a CHI600D electrochemical workstation with a platinum working electrode and a Pt wire counter electrode at a scan rate of 50 mV s^{-1} against an Ag/Ag^+ (0.1 M of $AgNO_3$ in acetonitrile) reference electrode with a nitrogen-saturated anhydrous solution of 0.1 mol L^{-1} tetrabutylammonium hexafluorophosphate (Bu_4NPF_6) in acetonitrile. The polymer films for electrochemical measurements were coated from a polymer−THF dilute solution.

Hole mobility was measured in hole-only devices by using the space charge limited current (SCLC) method[35,36] with a device configuration of Au/MoO_3/blend layer/PEDOT:PSS/ITO. The mobility were determined by fitting the dark current to the model of a single carrier SCLC with field-dependent mobility, which is described as

$$J = \frac{9}{8}\varepsilon_0\varepsilon_r\mu_0\frac{V^2}{L^3}$$

where J is the current, μ_0 is the zero-field mobility, ε_0 is the permittivity of free space, ε_r is the relative permittivity of the material, L is the thickness of the active layer, and V is the effective voltage. The effective voltage can be obtained by subtracting the built-in voltage (V_{BI}) and the voltage drop (V_{RS}) from the substrate's series resistance from the applied voltage (V_{APPL}), $V = V_{APPL} - V_{BI} - V_{RS}$. In every simulation, ε_r was assumed to be 3, which is a typical value for conjugated polymers. L = 75 nm, which was measured by using atomic force microscopy. The series resistance of the device was determined from the reference device without the active layer, i.e., a device configuration of Au/MoO_3/PEDOT:PSS/ITO, and was found to be ca. 10 Ω cm^{-2}. V_{BI} values of 0.10 and 0.10 V were used for devices with active materials PSiFDCN and PSiFDTA, respectively, which provided best fits to the $\log(J)-V$ curves. Variable parameter μ_0 was derived from the simulations.

Atom force microscopy (AFM) measurements were carried out using a Digita Instrumental DI Multimode Nanoscope IIIa in taping mode.

Solar Cell Device Fabrication and Characterization. ITO-coated glass substrates were cleaned by sonication in detergent, deionized water, acetone, and isopropyl alcohol and dried in a nitrogen stream, followed by an oxygen plasma treatment. To fabricate photovoltaic devices, a hole transport thin layer (ca. 40 nm) of PEDOT:PSS (Baytron P VP AI 4083, filtered at 0.45 μm)

Scheme 1. Synthetic Route of PSiFDCN and PSiFDTA

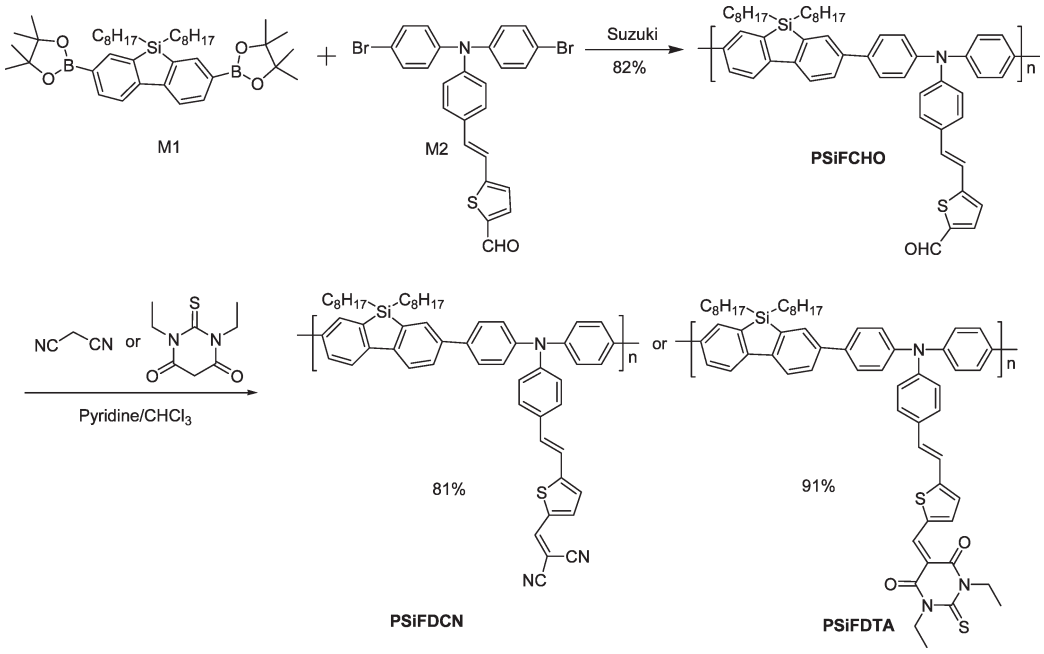

was spin-coated on the precleaned ITO-coated glass substrates at 5000 rpm and baked at 140 °C for 10 min under ambient conditions. The substrates were then transferred into an argon-filled glovebox. Subsequently, the polymer:$PC_{71}BM$ active layer (ca. 80 nm for PSiFDCN and 60 nm for PSiFDTA) was spin-coated on the PEDOT:PSS layer at 1000 rpm from a homogeneous blend solution. The solution was prepared by dissolving the polymers (2 mg mL^{-1}) and $PC_{71}BM$ (8 mg mL^{-1}) in a tetrahydrofuran/chlorobenzene (1/1, v/v) solvent mixture for PSiFDCN and chloroform/chlorobenzene (1/1, v/v) solvent mixture for PSiFDTA and filtered with a 0.2 μm PTFE filter. The substrates were annealed at 150 °C for 10 min prior to electrode deposition. To complete device fabrication, the substrates were pumped down to a high vacuum (1×10^{-6} Torr), and barium (4 nm) topped with aluminum (100 nm) was thermally evaporated onto the active layer through shadow masks. The effective devices area was measured to be 0.15 cm^2.

The current density−voltage ($J-V$) characteristics were recorded with a Keithley 236 source meter. The spectral response was measured with a commercial photomodulation spectroscopic setup (Oriel). A calibrated Si photodiode was used to determine the photosensitivity. The external quantum efficiency (EQE) of the devices was measured on a Hypermonolight System (Bunkoh-Keiki SM-250).

Results and Discussion

Synthesis and Characterization. The structures and the synthetic route to the polymers are outlined in Scheme 1. The two monomers M1 and M2 were prepared as in the literature.[22,33,34] The precursor polymer, PSiFCHO, was synthesized by Suzuki polycondensation of an equimolecular mixture of the two monomer, M1 and M2. The polymerization was carried out for 7 h using $Pd(PPh_3)_4$ as the catalyst in the two-phase mixture of toluene/tetrahydrofuran (1/1, v/v) and aqueous Na_2CO_3 (1.0 M). The two resultant polymers, PSiFDCN and PSiFDTA, were obtained by a Knoevenagel condensation between the aldehyde-functionalized conjugated precursor polymer and malononitrile and diethylthiobarbituric acid in the presence of pyridine, in 81% and 91% yield, respectively. The chemical structures of the polymers were verified by ^1H NMR and elemental analyses. The complete disappearances of the aromatic aldehyde proton signal at 9.85 ppm[37,38] and the appearances of olefinic proton signals at 7.74 ppm[37] for PSiFDCN and 8.62 ppm for PSiFDTA confirmed the efficient conversion reaction. The M_n of PSiFCHO determined by gel permeation chromatography (GPC) in THF using polystyrene as standard is 10.2 kg mol^{-1} with a polydispersity index (PDI) of 2.98. The modification has resulted in a slight increase in the molecular weights of the resulting polymers, as outlined in Table 1. The M_n of PSiFDCN and PSiFDTA are 11.5 and 12.3 kg mol^{-1}, with the corresponding PDI of 2.69 and 2.83, respectively. PSiFDTA has excellent solubility in common organic solvents such as THF, chloroform, and chlorobenzene due to its bulky side chain. The solubility of PSiFDCN is not good as PSiFDTA in chloroform and chlorobenzene, but it has good solubility in THF. Both polymers could be readily cast into uniform thin films, rendering them good candidates for the fabrication of PSCs devices.

Table 1. Molecular Weight and Thermal Properties of the Polymers

polymer	M_n (kg mol^{-1})	M_w (kg mol^{-1})	PDI	T_d (°C)	T_g (°C)
PSiFDCN	11.5	31.0	2.69	382	179
PSiFDTA	12.3	34.8	2.83	291	172

Thermal Properties. The thermal properties of PSiFDCN and PSiFDTA were determined by DSC and TGA under a nitrogen atmosphere. As shown in Figure 1 and Table 1, both polymers exhibited good thermal stability with 5% weight-loss temperatures (T_d) of 382 and 291 °C. The glass transition temperature (T_g) are 179 and 172 °C for PSiFDCN and PSiFDTA, respectively. No crystallization or melting peak is observed upon further heating beyond the T_g. The good thermal stability of the polymers retards the deformation of the polymer morphology and the degradation of the active layer at elevated temperatures, which are desirable for polymers in PSCs applications.[39]

Optical Properties. To investigate the photophysical properties of the polymers, the absorption spectra were recorded in both chloroform solution and thin films, which is shown in Figure 2 and Table 2. In solution, the polymers exhibit two distinct absorption bands, where the first absorption peaks

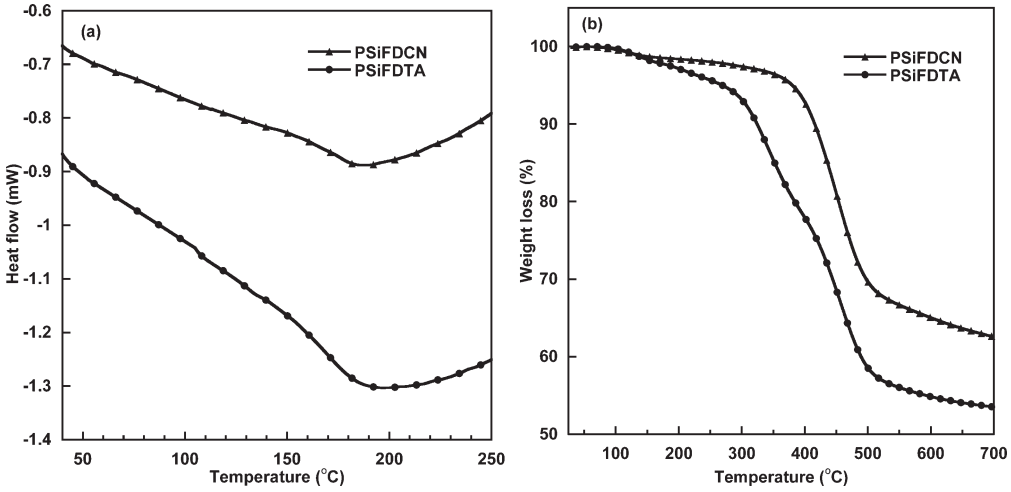

Figure 1. DSC plots (a) and TGA plots (b) of PSiFDCN and PSiFDTA.

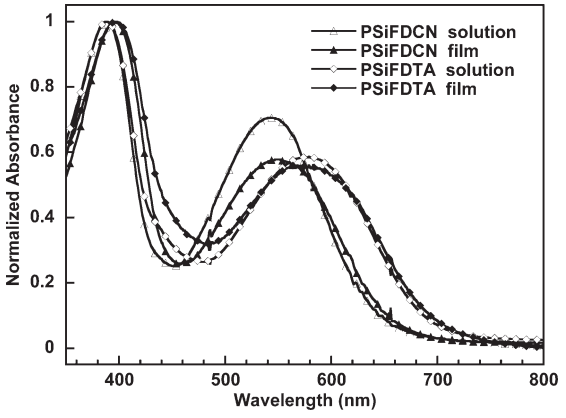

Figure 2. UV−vis absoption spectra of PSiFDCN and PSiFDTA.

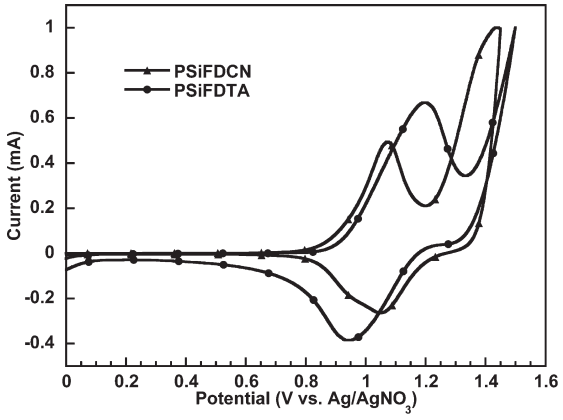

Figure 3. Cyclic voltammograms of the polymers films measured in 0.1 M Bu_4NPF_6 in acetonitrile at a scan rate of 50 mV s^{-1}.

Table 2. Electrochemical and Optical Properties of the Polymers

polymer	λ_{abs} (nm) solution	λ_{abs} (nm) film	E_g^{opt} (eV)	E_{ox} (V)	E_{HOMO} (eV)	E_{LUMO} (eV)
PSiFDCN	389 541	398 548	1.83	0.89	−5.32	−3.49
PSiFDTA	388 579	396 583	1.74	0.92	−5.35	−3.61

at ~388 nm are corresponding to the $\pi-\pi^*$ transition of their conjugated backbone[22,37] and the peaks at the longer wavelength could be attributed to the strong intramolecular charge transfer (ICT) interaction between their conjugated main chains and the pendant acceptor groups.[22,37,40] By using a stronger acceptor, PSiFDTA exhibits an obviously red-shifted ICT absorbance peak compared to PSiFDCN, which could be explained by much stronger ICT interaction in the PSiFDTA than that in PSiFDCN. The absorption spectra in the solid state of both polymers are slight red-shifted compared with the corresponding spectra in dilute solution, indicating the presence of intermolecular interactions in the solid state. The interaction seem to be not as strong as those of linear D−A type polymers, probably due to the bulky side chains retard the efficient packing of the polymer chains in the solid state. The optical band gaps (E_g^{opt}) of the two polymers calculated from the absorption onset in the films are 1.83 eV for PSiFDCN and 1.74 eV for PSiFDTA, respectively. Clearly, the photophysical properties and energy levels of the resultant polymers can be easily tuned by simply changing the strength of the acceptor in the side chains. The absorption spectra and band gap of the two silafluorene-based polymers are similar to that of their carbon bridging analogues,[22] indicating that the bridging atom has little influence on the photophysical properties of the polymers. This is consistent with our previous result that PSiFDBT has similar photophysical properties with its carbon bridging analogues PFDTBT. Additionally, it is worth noting that the styrylthiophene π-bridge at the side chains could significantly red-shift the absorption spectra by extending the conjugated length.[37,38]

Electrochemical Properties. To further understand the electronic structures of the polymers, and then provide key parameters for the design of PSCs devices, it is necessary to determine the energy levels of the HOMO and the lowest unoccupied molecular orbital (LUMO) of the conjugated polymers. Thus, the electrochemical characteristics of the polymers films on a Pt electrode were investigated by cyclic voltammetry (CV) with Bu_4NPF_6 (0.1 M in acetonitrile) as the electrolyte and Ag/Ag^+ (0.1 M of $AgNO_3$ in acetonitrile) electrode as reference electrode at a scan rate of 50 mV s^{-1}, and the results are summarized in Figure 3 and Table 2. Both polymers exhibit two obvious oxidation peaks: the first reversible one corresponds to the oxidation of the triphenylamine moiety, and the other is attributed to the oxidation of the silafluorene ring. To obtain accurate redox potentials, the reference electrode was calibrated by the ferrocene/ferrocenium (Fc/Fc^+), whose redox potential is assumed to have an absolute energy level of −4.80 eV to vacuum.[41] As a

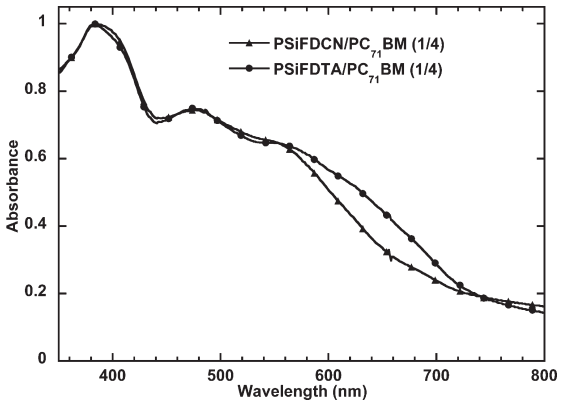

Figure 4. UV−vis absorption spectra of polymer:$PC_{71}BM$ (1:4) blend films.

result, the HOMO energy values were calculated using the equation

$$E_{HOMO} = -e(E_{ox} + 4.43)\ (eV)$$

where E_{ox} is the onset oxidation potential vs Ag/Ag^+. The HOMO energy values of PSiFDCN and PSiFDTA were calculated to be −5.32 and −5.35 eV, respectively. The LUMO energy levels of the polymers were estimated from the HOMO energy levels and E_g^{opt} using the equation

$$E_{LUMO} = E_{HOMO} + E_g^{opt}$$

due to the reduction curves could hardly be obtained, which is −3.49 and −3.61 eV, respectively.

It is worth noting that the HOMO levels of the polymers were not raised obviously despite the presence of different acceptors in side chains, and similar phenomena were also observed in triphenylamine-based small molecule solar cell materials.[40] Moreover, it has also been reported that the HOMO of triphenylamine-based small molecule solar cell materials can be effectively decreased by attaching electron-withdrawing acceptor groups.[40,42] Since V_{oc} of PSCs relates with the difference between the HOMO level of electron donor and the LUMO level of electron acceptor,[11] it was expected that PSCs based on PSiFDCN and PSiFDTA would have high V_{oc}. In addition, the offsets between the LUMO levels of both new polymers and $PC_{71}BM$ (−4.3 eV) are larger than 0.3 eV, indicating that charge transfer from the polymers to $PC_{71}BM$ would be efficient.[43,44]

Photovoltaic Properties. In order to investigate the potential application of PSiFDCN and PSiFDTA in PSCs, bulk heterojunction photovoltaic devices were fabricated with a sandwich structure of ITO/PEDOT:PSS/polymer:$PC_{71}BM$/Ba/Al. The $PC_{71}BM$ was chosen as the acceptor due to it has similar electronic properties as $PC_{61}BM$, but a higher absorption coefficient in the visible region with a broad peak from 440 to 530 nm, which could complement the absorption valley of the polymers,[45] as the absorption spectra of polymer:$PC_{71}BM$ shown in Figure 4. It was reported that PSCs based on similar polymers PFDCN and PFPDT exhibit best performance when the polymer:$PC_{71}BM$ blend films are prepared from mixed solvent of chloroform/chlorobenzene (1/1, v/v).[22] Therefore, chloroform/chlorobenzene (1/1, v/v) solvent mixture was used to prepare PSiFDTA:$PC_{71}BM$ blend films. However, PSiFDCN:$PC_{71}BM$ blend films were prepared from THF/chlorobenzene due to the poor solubility of PSiFDCN in chloroform and chlorobenzene.

Table 3. Photovoltaic Performance of the Polymers Measured under the Illumination of Simulated AM 1.5 G Conditions (800 W m^{-2})

polymer	V_{oc} (V)	J_{sc} (mA cm^{-2})	FF	PCE (%)
PSiFDCN	0.85	6.69	0.369	2.50
PSiFDTA	0.90	6.22	0.451	3.15

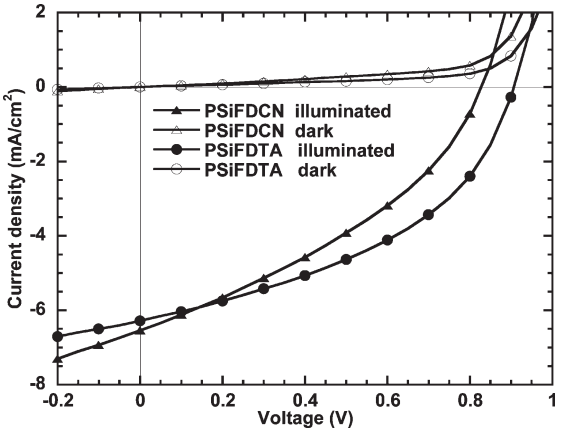

Figure 5. $J-V$ characteristics of the devices with the structure of ITO/PEDOT:PSS/polymer:$PC_{71}BM$ (1:4, w/w)/Ba/Al.

The $J-V$ characteristics of the cells based on PSiFDCN:$PC_{71}BM$ (1:4, w/w) and PSiFDTA:$PC_{71}BM$ (1:4, w/w) measured under the illumination of simulated AM 1.5 G conditions (800 W m^{-2}) are shown in Figure 5. The highest PCE of PSiFDCN:$PC_{71}BM$ solar cells reaches 2.50% with an open-circuit voltage (V_{oc}) of 0.85 V, a short-circuit current (J_{sc}) of 6.69 mA cm^{-2}, and a fill factor (FF) of 36.9%. A much higher PCE of 3.15% was observed from the solar cells made by PSiFDTA:$PC_{71}BM$ with a V_{oc} of 0.90 V, a J_{sc} of 6.22 mA cm^{-2}, and a FF of 45.1%. It is worth noting that the V_{oc} of PSiFDCN and PSiFDTA are comparable to the best data of the linear low-band-gap polymers based on silafluorene reported in the literature,[18,46] indicating that the HOMO levels of silafluorene-based two-dimensional polymers elevated little when incorporating electron-drawing moieties in side chains, which is in accordance with a previous report.[22]

The charge carriers transport properties of conjugated polymers play a key role in the performance of PSCs.[47] To understand the influence of charge carrier mobility in the blend films on the J_{sc} and FF, the hole mobility of the polymers is measured by using the SCLC method, which is extensively used to investigate the charge transport properties of the PSCs active layer.[35,36] The $J^{1/2}-V$ plots for the polymer:$PC_{71}BM$ blends are shown in Figure 6. Hole mobilities of 1.77×10^{-4} and 2.11×10^{-4} $cm^2\ V^{-1}\ s^{-1}$ are observed for PSiFDCN and PSiFDTA, respectively, which is comparable to those linear D−A conjugated polymers.[18,48] It should be pointed out that the mobility of these two silicon bridging polymers are slightly lower than that of their carbon bridging analogues PFDCN and PFDTA. This result is different from the general view that the mobility of the silicon bridging conjugated polymers are higher than their carbon analogues, which is widely observed in linear conjugated polymers.[13,18,49] Nevertheless, considering their two-dimensional conjugated characteristics, the better isotropic charge transport properties of PSiFDCN and PSiFDTA than linear polymers are beneficial for PSCs applications.[23−25]

The film morphology of the active layer is very important to the performance of PSCs.[50−52] Thus, the film morphology of polymer:$PC_{71}BM$ blends was studied. As the

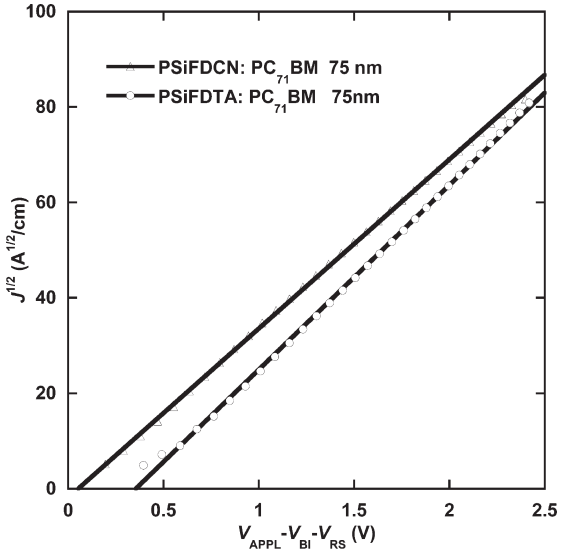

Figure 6. $J^{1/2}-V$ characteristics of devices in Au/MoO_3/polymer: $PC_{71}BM$/PEDOT:PSS/ITO configuration. The solid lines represent the fitting curves.

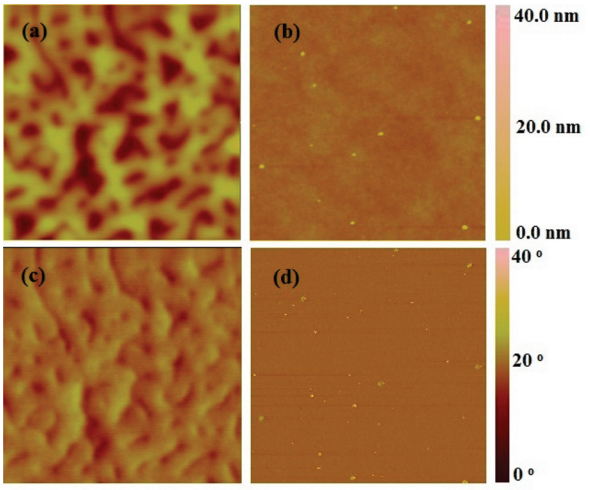

Figure 7. AFM images: (a) and (b) are height images for PSiFDCN and PSiFDTA, respectively; (c) and (d) are corresponding phase images for PSiFDCN and PSiFDTA, respectively. All the images are 5 μm × 5 μm.

tapping-mode AFM images shown in Figure 7, the surface of the active layers of PSiFDTA:$PC_{71}BM$ is quite smooth, with a root-mean-square roughness (rms) of 0.573 nm. However, the surface of the active layers of PSiFDCN:$PC_{71}BM$ is comparatively rough, with a rms of 3.655 nm. The films morphologies are in accordance with their surface roughness. The film of PSiFDCN:$PC_{71}BM$ exhibits distinct phase separation into islands with a large domain size of 500−1000 nm. The film of PSiFDTA:$PC_{71}BM$ exhibits good film morphology with a much smaller domain size, indicating a much more uniform mixing of PSiFDTA and $PC_{71}BM$, which is beneficial to obtain as large as interface areas and accordingly to maximize J_{sc} and FF. The different solvents (THF/chlorobenzene for PSiFDCN and chloroform/chlorobenzene for PSiFDTA) used to prepare the active layer films may be responsible for the films morphology difference of PSiFDCN:$PC_{71}BM$ and PSiFDTA:$PC_{71}BM$.[53] As a result, the PSC based on PSiFDTA exhibited much better device performance than that of the device based on PSiFDCN.

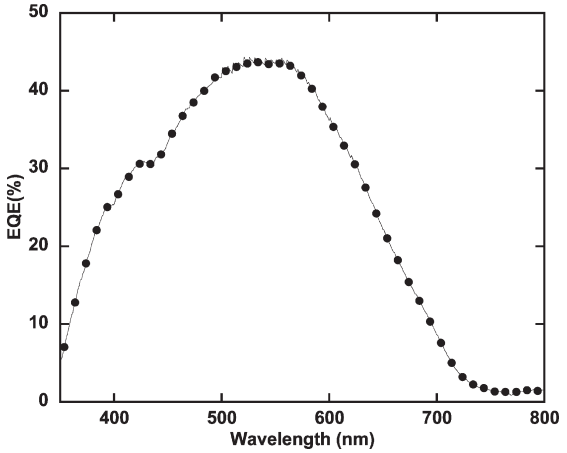

Figure 8. EQE spectrum of PSiFDTA-based solar cell illuminated by monochromatic light.

To confirm the PCE, the external quantum efficiency (EQE) of the device based on PSiFDTA illuminated by monochromatic light was determined. The device based on PSiFDTA exhibits very efficient photoresponse in the broad range from 350 to 750 nm as the EQE curve shown in Figure 8. The high EQE over 40% was observed in a very broad range from 482 to 587 nm with the maximum of 44.3% at 521 nm, reflecting the importance of the absorption complement of $PC_{71}BM$. The integral of the EQEs are in accordance with the J_{sc} measured from the devices.

Conclusion

In summary, two new silafluorene-based conjugated polymers PSiFDCN and PSiFDTA carrying strong pendant acceptor groups have been successfully synthesized. Both of them exhibit good solubility in common organic solvents and excellent thermal stability. The energy levels and band gap of the polymers could be effectively tuned by changing the strength of the acceptor groups in side chains. The bulk heterojunction polymer solar cells based on PSiFDCN and PSiFDTA exhibit promising power conversion efficiency of 2.50% and 3.15%, respectively. Moreover, different from most linear low-band-gap conjugated polymers, photovoltaic devices based on these two low-band-gap polymers still exhibit high V_{oc}. These results demonstrate that the two polymers are promising donor materials for high performance solar cells. Furthermore, if a stronger acceptor was attached to the side chain, a lower-band-gap polymer with an ideal energy level at the same time would be obtained, and consequently, a higher PCE could be anticipated.

Acknowledgment. The work was financially supported by the Natural Science Foundation of China (No. 50990065 and 20904011) and the Ministry of Science and Technology, China (MOST), and National Research Project (No. 2009CB623601). F. Huang thanks the Fundamental Research Funds for the Central Universities, South China University of Technology (No. 2009220012), for financial support.

References and Notes

(1) Yu, G.; Gao, J.; Hummelen, J. C.; Wudl, F.; Heeger, A. J. *Science* **1995**, *270*, 1789–1791.
(2) Brabec, C. J.; Sariciftci, N. S.; Hummelen, J. C. *Adv. Funct. Mater.* **2001**, *11*, 15–26.
(3) Gunes, S.; Neugebauer, H.; Sariciftci, N. S. *Chem. Rev.* **2007**, *107*, 1324–1338.
(4) Thompson, B. C.; Frechet, J. M. J. *Angew. Chem., Int. Ed.* **2008**, *47*, 58–77.

(5) Helgesen, M.; Sondergaard, R.; Krebs, F. C. *J. Mater. Chem.* **2010**, *20*, 36–60.
(6) Chen, J.; Cao, Y. *Acc. Chem. Res.* **2009**, *42*, 1709–1718.
(7) Wienk, M. M.; Kroon, J. M.; Verhees, W. J. H.; Knol, J.; Hummelen, J. C.; van Hal, P. A.; Janssen, R. A. J. *Angew. Chem., Int. Ed.* **2003**, *42*, 3371–3375.
(8) Li, Y. F.; Zou, Y. P. *Adv. Mater.* **2008**, *20*, 2952–2958.
(9) Cheng, Y.-J.; Yang, S.-H.; Hsu, C.-S. *Chem. Rev.* **2009**, *109*, 5868–5923.
(10) Kroon, R.; Lenes, M.; Hummelen, J. C.; Blom, P. W. M.; De Boer, B. *Polym. Rev.* **2008**, *48*, 531–582.
(11) Scharber, M. C.; Wuhlbacher, D.; Koppe, M.; Denk, P.; Waldauf, C.; Heeger, A. J.; Brabec, C. J. *Adv. Mater.* **2006**, *18*, 789–794.
(12) Peet, J.; Kim, J. Y.; Coates, N. E.; Ma, W. L.; Moses, D.; Heeger, A. J.; Bazan, G. C. *Nat. Mater.* **2007**, *6*, 497–500.
(13) Hou, J.; Chen, H.-Y.; Zhang, S.; Li, G.; Yang, Y. *J. Am. Chem. Soc.* **2008**, *130*, 16144–16145.
(14) Liang, Y.; Wu, Y.; Feng, D.; Tsai, S.-T.; Son, H.-J.; Li, G.; Yu, L. *J. Am. Chem. Soc.* **2008**, *131*, 56–57.
(15) Liang, Y.; Feng, D.; Wu, Y.; Tsai, S.-T.; Li, G.; Ray, C.; Yu, L. *J. Am. Chem. Soc.* **2009**, *131*, 7792–7799.
(16) Hou, J.; Chen, H.-Y.; Zhang, S.; Chen, R. I.; Yang, Y.; Wu, Y.; Li, G. *J. Am. Chem. Soc.* **2009**, *131*, 15586–15587.
(17) Chen, H. Y.; Hou, J. H.; Zhang, S. Q.; Liang, Y. Y.; Yang, G. W.; Yang, Y.; Yu, L. P.; Wu, Y.; Li, G. *Nat. Photonics* **2009**, *3*, 649–653.
(18) Wang, E. G.; Wang, L.; Lan, L. F.; Luo, C.; Zhuang, W. L.; Peng, J. B.; Cao, Y. *Appl. Phys. Lett.* **2008**, *92*, 033307.
(19) Park, S. H.; Roy, A.; Beaupre, S.; Cho, S.; Coates, N.; Moon, J. S.; Moses, D.; Leclerc, M.; Lee, K.; Heeger, A. J. *Nat. Photonics* **2009**, *3*, 297–303.
(20) Qin, R.; Li, W.; Li, C.; Du, C.; Veit, C.; Schleiermacher, H.-F.; Andersson, M.; Bo, Z.; Liu, Z.; Inganas, O.; Wuerfel, U.; Zhang, F. *J. Am. Chem. Soc.* **2009**, *131*, 14612–14613.
(21) Wong, W. Y.; Wang, X. Z.; He, Z.; Djurisic, A. B.; Yip, C. T.; Cheung, K. Y.; Wang, H.; Mak, C. S. K.; Chan, W. K. *Nat. Mater.* **2007**, *6*, 521–527.
(22) Huang, F.; Chen, K.-S.; Yip, H.-L.; Hau, S. K.; Acton, O.; Zhang, Y.; Luo, J.; Jen, A. K. Y. *J. Am. Chem. Soc.* **2009**, *131*, 13886–13887.
(23) Roncali, J.; Leriche, P.; Cravino, A. *Adv. Mater.* **2007**, *19*, 2045–2060.
(24) Wang, Y.; Zhou, E.; Liu, Y.; Xi, H.; Ye, S.; Wu, W.; Guo, Y.; Di, C.-A.; Sun, Y.; Yu, G.; Li, Y. *Chem. Mater.* **2007**, *19*, 3361–3363.
(25) Zhou, E. J.; Tan, Z.; Yang, C. H.; Li, Y. F. *Macromol. Rapid Commun.* **2006**, *27*, 793–798.
(26) Hou, J. H.; Tan, Z. A.; Yan, Y.; He, Y. J.; Yang, C. H.; Li, Y. F. *J. Am. Chem. Soc.* **2006**, *128*, 4911–4916.
(27) Blouin, N.; Michaud, A.; Leclerc, M. *Adv. Mater.* **2007**, *19*, 2295–2300.
(28) Svensson, M.; Zhang, F. L.; Veenstra, S. C.; Verhees, W. J. H.; Hummelen, J. C.; Kroon, J. M.; Inganas, O.; Andersson, M. R. *Adv. Mater.* **2003**, *15*, 988–991.
(29) Muhlbacher, D.; Scharber, M.; Morana, M.; Zhu, Z. G.; Waller, D.; Gaudiana, R.; Brabec, C. *Adv. Mater.* **2006**, *18*, 2884–2889.
(30) Yue, W.; Zhao, Y.; Shao, S. Y.; Tian, H. K.; Xie, Z. Y.; Geng, Y. H.; Wang, F. S. *J. Mater. Chem.* **2009**, *19*, 2199–2206.
(31) Scharber, M. C.; Koppe, M.; Gao, J.; Cordella, F.; Loi, M. A.; Denk, P.; Morana, M.; Egelhaaf, H. J.; Forberich, K.; Dennler, G.; Gaudiana, R.; Waller, D.; Zhu, Z. G.; Shi, X. B.; Brabec, C. J. *Adv. Mater.* **2010**, *22*, 367–370.
(32) Chen, H. Y.; Hou, J. H.; Hayden, A. E.; Yang, H.; Houk, K. N.; Yang, Y. *Adv. Mater.* **2010**, *22*, 371–375.
(33) Chan, K. L.; McKiernan, M. J.; Towns, C. R.; Holmes, A. B. *J. Am. Chem. Soc.* **2005**, *127*, 7662–7663.
(34) Wang, E.; Li, C.; Peng, J.; Cao, Y. *J. Polym. Sci., Part A: Polym. Chem.* **2007**, *45*, 4941–4949.
(35) Malliaras, G. G.; Salem, J. R.; Brock, P. J.; Scott, C. *Phys. Rev. B* **1998**, *58*, 13411–13414.
(36) Goh, C.; Kline, R. J.; McGehee, M. D.; Kadnikova, E. N.; Frechet, J. M. J. *Appl. Phys. Lett.* **2005**, *86*, 122110.
(37) Zhang, Z.-G.; Zhang, K.-L.; Liu, G.; Zhu, C.-X.; Neoh, K.-G.; Kang, E.-T. *Macromolecules* **2009**, *42*, 3104–3111.
(38) Zhang, W.; Fang, Z.; Su, M. J.; Saeys, M.; Liu, B. *Macromol. Rapid Commun.* **2009**, *30*, 1533–1537.
(39) Li, J. Y.; Liu, D.; Li, Y. Q.; Lee, C. S.; Kwong, H. L.; Lee, S. T. *Chem. Mater.* **2005**, *17*, 1208–1212.
(40) Leriche, P.; Frere, P.; Cravino, A.; Aleveque, O.; Roncali, J. *J. Org. Chem.* **2007**, *72*, 8332–8336.
(41) Pommerehne, J.; Vestweber, H.; Guss, W.; Mahrt, R. F.; Bassler, H.; Porsch, M.; Daub, J. *Adv. Mater.* **1995**, *7*, 551–554.
(42) Roquet, S.; Cravino, A.; Leriche, P.; Aleveque, O.; Frere, P.; Roncali, J. *J. Am. Chem. Soc.* **2006**, *128*, 3459–3466.
(43) Sariciftci, N. S.; Smilowitz, L.; Heeger, A. J.; Wudl, F. *Science* **1992**, *258*, 1474–1476.
(44) Kraabel, B.; McBranch, D.; Sariciftci, N. S.; Moses, D.; Heeger, A. J. *Phys. Rev. B* **1994**, *50*, 18543.
(45) Yao, Y.; Shi, C.; Li, G.; Shrotriya, V.; Pei, Q.; Yang, Y. *Appl. Phys. Lett.* **2006**, *89*, 153507.
(46) Boudreault, P. L. T.; Michaud, A.; Leclerc, M. *Macromol. Rapid Commun.* **2007**, *28*, 2176–2179.
(47) Blom, P. W. M.; Mihailetchi, V. D.; Koster, L. J. A.; Markov, D. E. *Adv. Mater.* **2007**, *19*, 1551–1566.
(48) Huo, L. J.; Chen, H. Y.; Hou, J. H.; Chen, T. L.; Yang, Y. *Chem. Commun.* **2009**, 5570–5572.
(49) Zhu, Z.; Waller, D.; Gaudiana, R.; Morana, M.; Muhlbacher, D.; Scharber, M.; Brabec, C. *Macromolecules* **2007**, *40*, 1981–1986.
(50) Hoppe, H.; Sariciftci, N. S. *J. Mater. Chem.* **2006**, *16*, 45–61.
(51) Yang, X.; Loos, J. *Macromolecules* **2007**, *40*, 1353–1362.
(52) Moule, A. J.; Meerholz, K. *Adv. Funct. Mater.* **2009**, *19*, 3028–3036.
(53) Zhang, F. L.; Jespersen, K. G.; Bjorstrom, C.; Svensson, M.; Andersson, M. R.; Sundstrom, V.; Magnusson, K.; Moons, E.; Yartsev, A.; Inganas, O. *Adv. Funct. Mater.* **2006**, *16*, 667–674.